Changes in Polypeptide Initiation and Elongation Rates during the Cell Cycle of *Chlamydomonas reinhardi*†

D. Mona Baumgartel and Stephen H. Howell*

ABSTRACT: Changes in the rate of protein synthesis during the cell cycle of *Chlamydomonas reinhardi* have been measured by determining changes in the separate rates of polypeptide chain initiation and elongation and in the rate of incorporation of a radioactive amino acid. The rate of polypeptide chain elongation, determined from the relative rates of labeling of two size classes of polyribosomes, varies only about twofold during the cell cycle. The rate of polypeptide chain initiation, determined from an analysis of the distribution of ribosomes in monoribosomes (and ribosomal subunits) and polyribosomes, varies more than 25-fold. Also, the overall rate of protein synthesis during the cell cycle varies to the same extent as the rate of chain initiation. Measurement of protein synthetic rates using incorporation of a radioactive amino acid ([^{3}H]arginine) underestimates the actual change in the rate of protein synthesis during the cell cycle. The vast changes in the initiation rate during the cell cycle suggest a mechanism for selecting specific messenger RNAs for translation at different cell-cycle stages.

The cell cycle in many eucaryotic cells is marked by the periodic occurrence of cytological and biochemical events (see review: Mitchison, 1971). These events are easily studied in *Chlamydomonas reinhardi* which can be synchronized in the cell cycle by alterating light–dark illumination cycles.

Among the more recent cell-cycle events to be described in *C. reinhardi* are the stage-specific labeling (or synthesis) of major cellular polypeptides (Beck and Levine, 1974; Iwanij et al., 1975; Bourguignon and Palade, 1976; Howell et al., 1977). Howell et al. (1977) showed that 20 out of about 100 major cellular polypeptides are synthesized at independent rates during the cell cycle and in a stage-specific fashion, while the remaining polypeptides are synthesized throughout the cell cycle at rates commensurate with total protein synthesis. During the cell cycle, the rate of synthesis of any particular polypeptide could be regulated at many different levels which involve either transcriptional, posttranscriptional, or translational mechanisms. In this study, we will be concerned with changes in the efficiency of the translational machinery during the cell cycle and, in particular, the changes in rates of two component processes of protein synthesis, polypeptide chain initiation, and elongation.

Studies of other synchronized cell systems have shown that the rate of protein synthesis varies during the cell cycle. In cultured mammalian cells (Johnson and Holland, 1965; Steward et al., 1968; Fan and Penman, 1970), the rate of protein synthesis is lower in cells arrested in mitosis than in unblocked cells which are mostly in interphase. The drop in the rate of protein synthesis at mitosis has been attributed to a decrease in the rate of polypeptide chain initiation (Fan and Penman, 1970). The rate of protein synthesis also falls at mitosis in the slime mold *Physarum;* however, this change is thought to be caused by changes in the polypeptide elongation rate and not the initiation rate (Mittermayer et al., 1966; Brewer, 1972).

In this paper, we have studied the rates of protein synthesis at different cell-cycle stages in synchronous cultures of *C. reinhardi*. We have done so by evaluating the independent rates of polypeptide chain initiation[1] and elongation throughout the cell cycle. We have found that this method of measuring protein synthesis, using polyribosomes from different stages in the cell cycle, gives different results from and is more reliable than measuring rates of total amino acid incorporation.

Materials and Methods

Growth of Cells. A cell-wall-defective strain of *C. reinhardi,* CW2 mt$^-$ (generously provided by D. R. Davies), was used for these experiments. Cells were grown autotrophically in high-salt medium, 3/10 HSM (Sueoka et al., 1967), and bubbled with 3% CO_2 in air. Asynchronous cultures were maintained at 23–25 °C and illuminated constantly at a light intensity of 4000 lx at the culture surface. Cells were synchronized by subjecting cultures at 21 °C to a 12-h light–12-h dark illumination cycle. Light intensity during the light phase was 7000 lx at the culture surface.

Buffers and Reagents. Buffers used for polyribosome isolation were freshly prepared and autoclaved. Buffers used were: high-salt extraction buffer (high-salt EB[2]): 25 mM Tris-HCl (pH 7.5), 172 mM KCl, 28 mM KOH, 25 mM Na_2EDTA, 50 mM magnesium acetate, 1 mM 2-mercaptoethanol, 10 μg/mL polyvinyl sulfate (final total pH: 7.5); high-salt gradient buffer (high-salt GB): 25 mM Tris-HCl (pH 7.5), 200 mM KCl, 10 mM magnesium acetate, 1 mM 2-mercaptoethanol, 10 μg/mL polyvinyl sulfate.

All radioactive labeling was carried out using [3-^{3}H]arginine (New England Nuclear) at 10–20 Ci/mmol.

Uptake and Incorporation Measurements. Cultures were pulse labeled with [^{3}H]arginine as described in the figure legends. Uptake of [^{3}H]arginine by whole cells was measured by collecting 2 mL of labeled culture on glass-fiber filters and washing the cells rapidly with about 20 mL of 3/10 HSM

† From the Department of Biology, University of California, San Diego, La Jolla, California 92093. *Received August 3, 1976.* This work was supported by a grant from the National Science Foundation (GB-30237).

[1] Note use of the term *initiation rate,* r_i, defined in eq 2 under Discussion as the number of polypeptide chain-initiation events *per cell* per unit time, not per messenger RNA molecule or per ribosome per unit time.

[2] Abbreviations used are: EB, extraction buffer; GB, gradient buffer; Tris, 2-amino-2-hydroxymethyl-1,3-propanediol; EDTA, (ethylenedinitrilo)tetraacetic acid.

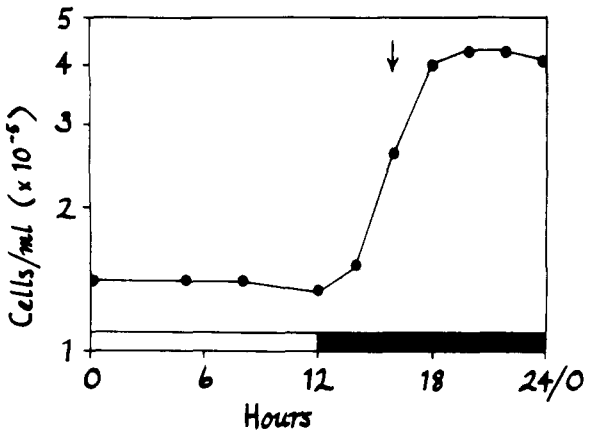

FIGURE 1: Synchronous division of *C. reinhardi* culture subjected to 12-h light (light bar)–12-h dark (dark bar) illumination cycles. Two milliliter samples were taken at the times indicated and cell density (cells/mL) was determined by hemacytometer counting. Time indicates the number of hours elapsed since the beginning of the light period. Arrow indicates the midpoint of the period of cell division.

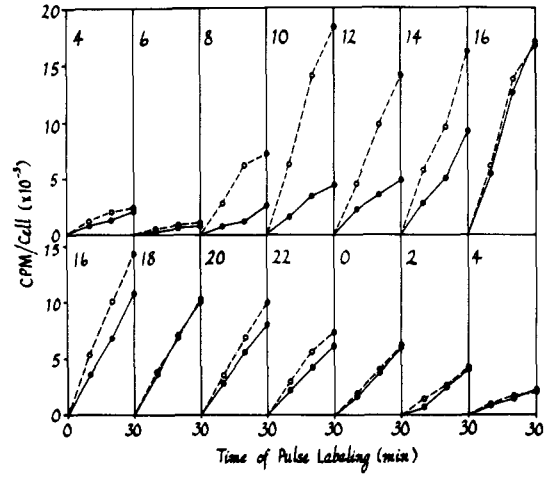

FIGURE 2: Uptake and incorporation of [^{3}H]arginine in synchronized *C. reinhardi* cultures. The cycle time designation on each panel refers to the number of hours elapsed since the beginning of the light period. Samples (13 mL) of cells were taken at 2-h intervals from two different synchronous cultures (upper and lower figures) and incubated in the light with 0.1 μCi/mL [^{3}H]arginine. Two 2-mL aliquots were removed from the incubating cultures at the times indicated and tested for [^{3}H]arginine uptake (O - - - O) or incorporation (●—●) as described under Materials and Methods.

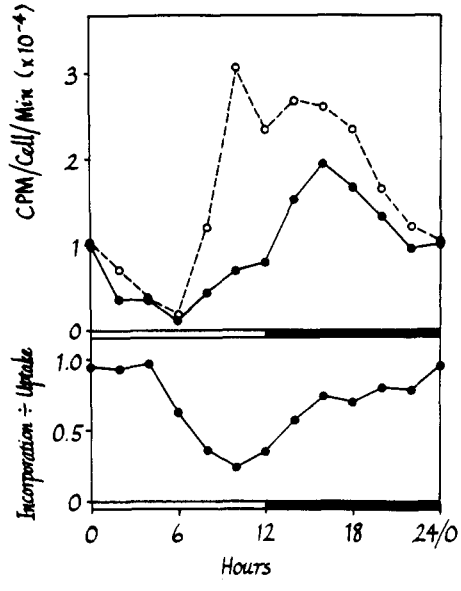

FIGURE 3: Rates of uptake and incorporation of [^{3}H]arginine during the cell cycle in synchronized *C. reinhardi* cultures using data from Figure 2. Cells were synchronized by a 12-h light (open bar)–12 h dark (closed bar) illumination cycle, and cell division occurred at about 16 h, as in Figure 1. Upper panel shows uptake (O - - - O) and incorporation (●—●) rates during the cell cycle. Lower panel shows ratio of incorporation and uptake rates.

containing 10 mM unlabeled arginine. The filters were dried and radioactivity was determined by scintillation counting. To minimize the effect of quenching of ^{3}H radioactivity by cellular material, fewer than 2×10^6 cells per filter were assayed.

Incorporation of [^{3}H]arginine by whole cells was measured by cold trichloroacetic acid precipitation of labeled cells. At the different time points, 1–2 mL of labeled culture was added to an equal volume of cold 20% trichloroacetic acid. After 15 min, the precipitated samples were collected on glass-fiber filters. The filters were washed with about 20 mL of cold 5% trichloroacetic acid and with 95% ethanol. Incorporation of [^{3}H]arginine into polyribosomal fractions was measured in the same way following acid precipitation. Polyribosomes were isolated according to Baumgartel and Howell (1976a), as described in Figure 4.

Polyacrylamide Gel Electrophoresis of Ribosomal RNA. Ribosomal RNA in polyribosomal fractions was analyzed by polyacrylamide gel electrophoresis. All procedures, including RNA extraction and electrophoresis, were carried out at 4 °C or below to preserve ribosomal RNA secondary structure (Cattolico and Jones, 1972). Pooled sucrose density gradient fractions were brought to 1% in sodium lauryl sulfate (Sigma), and an equal volume of 1:1 mixture of phenol–chloroform was added. The mixture was shaken for 15 min and centrifuged for 10 min at 10 000 rpm (Sorvall, SS-34 rotor). The upper phase was removed, mixed with 2 volumes of 95% ethanol, and stored at −20 °C overnight. The precipitated RNA was collected by centrifugation, and the pellet was air-dried. The RNA pellet was dissolved in a small volume of gel buffer containing 36 mM Tris, 30 mM NaH_2PO_4 and 1 mM Na_2EDTA (final pH 7.7) (Loening, 1969). Samples (containing 10–40 μg of RNA) were loaded onto 0.6-cm cylindrical 2.8% polyacrylamide gels. The samples were subjected to electrophoresis for 4 h at 5 mA/tube. Gels were scanned at 260 nm in a Gilford spectrophotometer equipped with a linear-transport mechanism.

Results

Uptake and Incorporation Rates. When *C. reinhardi* cells are subjected to a 12-h light–12-h dark illumination cycle, they will divide synchronously. Under the conditions used in this study, cell division (observed as an increase in cell density) typically occurred between 14 and 18 h, with a midpoint for the increase in cell density at about 16 h (Figure 1).

[^{3}H]Arginine is readily taken up and incorporated by *C. reinhardi* cells in asynchronous cultures. When synchronously grown cells were tested for their ability to utilize [^{3}H]arginine, it was found that the rates of uptake into the cells and incorporation into protein vary during the cell cycle (Figure 2). Although the rates are variable, both uptake and incorporation proceed approximately linearly from the time of addition of [^{3}H]arginine at nearly all cell-cycle stages. Thus, the arginine pool used for protein synthesis is rapidly equilibrated following addition of exogenous [^{3}H]arginine even when the rate of uptake is low. Figure 3 shows that the rate of [^{3}H]arginine incorporation keeps pace with the rate of uptake both early

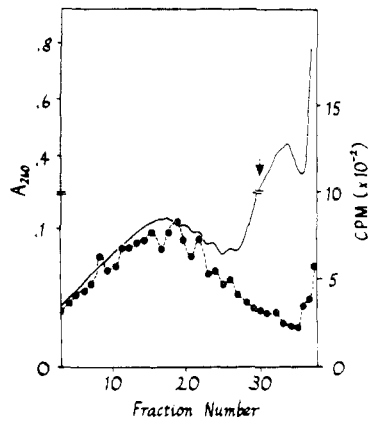

FIGURE 4: Polyribosome profile from asynchronous *C. reinhardi* cells. Cells were pulse labeled for 30 s with [^{3}H]arginine (0.1 μCi/mL) and immediately poured over sterile crushed ice. The cells were rapidly collected by centrifugation and resuspended in a small volume of high-salt EB containing 0.25 M sucrose. The cells were lysed in Nonidet P.40 at a final concentration of 2%, and the lysate was layered over a 15–30% sucrose gradient in high-salt GB. The gradient was centrifuged for 70 min at 41 rpm in a Beckman SW41 rotor at 4 °C. The optical density (A_{260}) profile (—) was analyzed using a flow cell in a Gilford Model 2400 spectrophotometer. Collected fractions were assayed for acid-precipitable radioactivity as described under Materials and Methods. The arrow shows the position of cytoplasmic monoribosomes on a similar gradient.

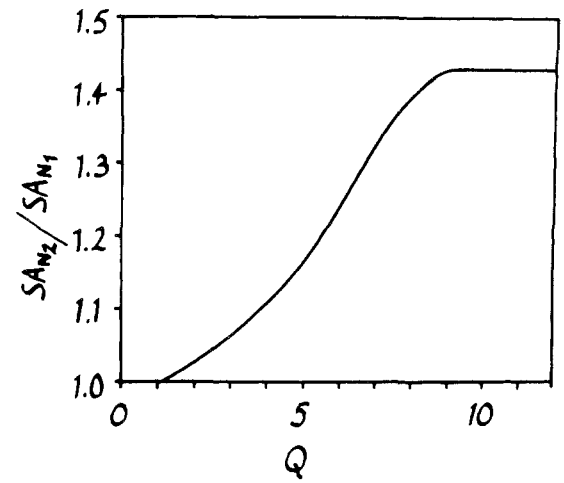

FIGURE 5: Theoretical plot of the ratio of nascent chain specific activities of two size classes of polyribosomes (SA_{N_2}/SA_{N_1}) vs. the number of peptide interval units completed during pulse labeling (Q). The expected specific activities of polyribosome size classes (SA: cpm in nascent chains/A_{260} in ribosomal RNA) have been derived from an analysis based on that of Kuff and Roberts (1967). According to that analysis, if all peptide interval units are uniformly labeled (where a peptide interval unit is the amount of nascent chain synthesized as a ribosome traverses a messenger RNA a distance equal to the average center to center spacing of adjacent ribosomes), then $SA = k[(N + 1)/2]$. The value of the parameter k depends on the specific activity of nascent peptide and the relationship between A_{260} and amount of ribosomes. It is assumed that the specific activity of the amino acid precursor pool is unchanging throughout the pulse so that k is constant. At labeling saturation, when all peptide intervals are labeled, having been synthesized during the pulse-labeling period, the ratio of specific activities of polyribosomes of sizes N_1 and N_2 (where $N_2 > N_1$) is: $SA_{N_2}/SA_{N_1} = (N_2 + 1)/(N_1 + 1)$. If, however, not all nascent chains are labeled, then the ratio is smaller. Before labeling saturation, the ratio increases as a function of the time required to synthesize a peptide interval unit, I, in the pulse-labeling time, t. Let Q be the number of peptide interval units synthesized during a pulse; thus, $Q = t/I$. Polyribosome specific activity can be expressed as a function of Q as follows: $SA = k[Q + (Q - Q^2)/2N]$, in unsaturated polyribosomes for which $Q < N$. Thus, the ratio of specific activities of two sizes of polyribosomes depends on whether or not either size class is fully labeled. If neither is saturated, that is, $Q < N_1$, then $SA_{N_2}/SA_{N_1} = N_1(2N_2 - Q + 1)/N_2(2N_1 - Q + 1)$, and, if the smaller polyribosomes are saturated while the larger ones are not ($N_1 \leq Q < N_2$), then $SA_{N_2}/SA_{N_1} = Q(2N_2 - Q + 1)/N_2(N_1 + 1)$. In this figure, these ratios of polyribosome specific activities are plotted as a function of increasing Q for $N_1 = 6$ and $N_2 = 9$.

(until 6 h) and late in the cell cycle (after 18 h), but near the light–dark transition (between 10 and 14 h) the rate of uptake exceeds the rate of incorporation. The ratio of incorporation and uptake rates during the cell cycle is presented in the lower part of Figure 3. This changing incorporation-to-uptake ratio suggests that the intracellular arginine pool used for protein synthesis is diluted to different extents during pulse labeling at different cell-cycle stages and that, therefore, the pool size also varies during the cell cycle. If the pool size varies and the rate of entry of [^{3}H]arginine into the pool changes also, then the specific activity of the pool following addition of [^{3}H]-arginine must also vary during the cell cycle. Variability in the pool specific activity means that total incorporation rates cannot be used to compare rates of protein synthesis.

The rate of [^{3}H]arginine incorporation varies tenfold during the cell cycle (Figure 3, top) and peaks early in the dark period (at 16 h). The rate of uptake of [^{3}H]arginine varies 15-fold and is highest during a broad period of the light–dark transition (from 10–18 h). We will return in a later section to a comparison of changes in the rate of [^{3}H]arginine incorporation during the cell cycle with changes in the actual rate of protein synthesis.

Nascent Polypeptide Chain Labeling Experiments. In the following sections, we show determinations of the rates of protein synthesis during the cell cycle using means which circumvent precursor-pool specific-activity problems. We have chosen to use analyses of polyribosomes to determine rates of polypeptide chain initiation and elongation. To determine elongation rates, we used a technique similar to that described by Enger and Tobey (1972) to measure rates of nascent polypeptide chain labeling. Basically, this involves comparing the rates of accumulation of nascent chain label in two size classes of polyribosomes. The measurements are unaffected by variable precursor pool specific activities in cells, for example, at different cell-cycle stages because the comparison is of the rates of chain labeling on different size classes of polyribosomes presumably utilizing the same precursor pool.

Asynchronous cells can be used to demonstrate the incorporation of label into nascent polypeptide following pulse labeling with [^{3}H]arginine. When polyribosomes from pulse-labeled cells are sedimented on sucrose density gradients, a polyribosomal profile such as that shown in Figure 4 is found. In the optical-density pattern, the smaller polyribosomes appear as distinct peaks (fractions 18–26) representing polyribosomes of from 2 to 7 ribosomes ($N = 2$ to $N = 7$). The expected sedimentation of higher-ordered polyribosomes ($N > 7$) has been extrapolated from the relationship between the log of the distance sedimented vs. log N of known polyribosomes (Morton, 1974; Reisner et al., 1972). Figure 4 shows that radioactivity from a 30-s [^{3}H]arginine pulse label is associated exclusively with polyribosomes, indicating that little breakdown of polyribosomes into monoribosomes has occurred. Also, the [^{3}H]arginine-labeled material is in nascent polypeptide chains, not in ribosomal proteins, as can be demonstrated by the complete "turnover" of label following a brief chase in the presence of excess unlabeled arginine (Baumgartel and Howell, 1976a). Although the polyribosomes are obtained from whole-cell preparations and include, therefore, both cytoplasmic and organellar (mostly chloroplastic) polyribosomes, the chloroplastic polyribosomes are small and are generally confined to the region of $N < 6$ in the polyribosomal profile

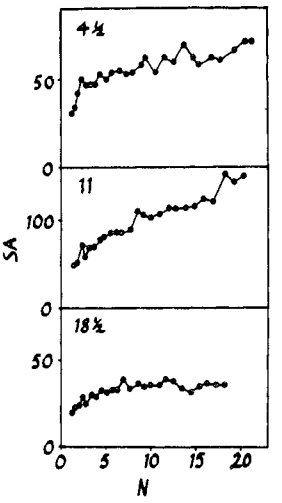

FIGURE 6: Specific activity (SA) vs. polyribosome size (N) plots for polyribosomes obtained from synchronized cells pulse labeled for 30 s with [^{3}H]arginine. Polyribosomes were extracted and analyzed as in Figure 4, and specific activities (SA: cpm in nascent polypeptide chains/A_{260} in ribosomal RNA) were determined for different size classes of polyribosomes. The different panels are from cells labeled at different times in the 12-h light–12 h dark illumination cycle. The designation on each panel refers to the number of hours after the lights go on in the 24-h cycle.

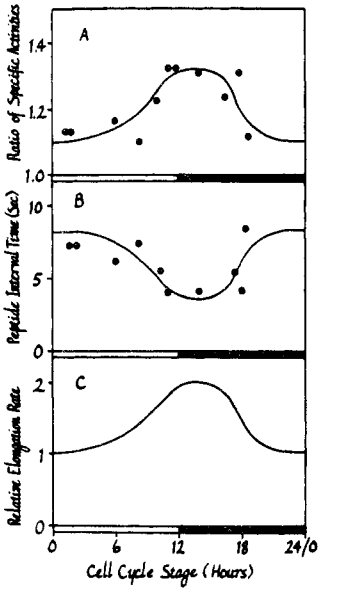

FIGURE 7: Ratio of specific activities of two size classes of polyribosomes from synchronized cultures pulsed labeled at different cell-cycle stages (panel A). Panel A shows the ratio of specific activities of polyribosomes of $N_2 = 9$ and $N_1 = 6$ obtained from SA vs. N plots described in Figure 5. Cells were pulse labeled for 30 s with [^{3}H]arginine at different times in the 12-h light (open bar)–12-h dark (closed bar) illumination cycle. The points were obtained from the analyses of separate, synchronous cell cultures sampled once or several times. Panel B shows peptide interval time, I, calculated according to eq 1. Panel B shows the inverse of the peptide interval time, or the relative elongation rate.

(Baumgartel and Howell, 1976a). Thus, the labeling of nascent chains in polyribosomes of $N > 6$ is due primarily to cytoplasmic, and not chloroplastic, protein synthesis. The matter of the size of chloroplast polyribosomes has been discussed previously (Baumgartel and Howell, 1976a) and will be dealt with more fully in a later section.

In order to use nascent chain labeling kinetics to determine rates of polypeptide chain elongation, we have compared the accumulation of nascent chain label in two size classes of polyribosomes. Since the amount of nascent chain per ribosome in polyribosomes increases with polyribosome size (Kuff and Roberts, 1967), the ratio of the labeled nascent chain contents per ribosome or specific activity (cpm in nascent polypeptide chains/A_{260} in ribosomal RNA) in two size classes of polyribosomes should increase with time of pulse labeling with a radioactive amino acid according to the relationship shown in Figure 5 (see figure legend for derivation and discussion). The ratio of specific activities will be 1.0 when only a small amount of peptide is synthesized during the pulse (when Q, in peptide interval units, as defined in Figure 5, is no greater than 1). If more peptide is synthesized during the pulse (higher Q), the specific-activity ratio increases and reaches a maximum when the larger polyribosome is fully labeled. One can use this relationship to determine the amount of peptide synthesized by cells with different elongation rates from the ratio of the accumulation of nascent chain label in two classes of polyribosomes and comparison of that ratio with the expected relationship shown in Figure 5. Therefore, the peptide interval time, I (the time required to fully label the peptide in one peptide interval unit), can be determined, since $I = t/Q$, where t is the pulse-labeling time.

In order to make this determination in synchronous cells at different cell-cycle stages, we used a constant pulse-labeling time of 30 s, since we have found that 30 s is not long enough in asynchronous cells to label the nascent chains of most classes of polyribosomes to saturation (Baumgartel and Howell, 1976b). We used the ratios of the specific activities of polyribosomes of $N_1 = 6$ and $N_2 = 9$. (The maximum ratio equals 1.43 at $Q \geq 9$.) These two size classes of polyribosomes were chosen for experimental measurements because the specific activities of the intermediate-sized polyribosomes can be accurately determined and because, in asynchronous cells, polyribosomes in these size classes accumulate nascent chain label according to the relationship shown in Figure 5. (Smaller and larger polyribosomes show certain anomalies in labeling, as discussed elsewhere (Baumgartel and Howell, 1976b).)

Plots of polyribosome specific activity from a few typical experiments with synchronous cultures are shown in Figure 6. The specific activities of various size classes of polyribosomes labeled at different cell-cycle stages (4.5, 11, and 18.5 h after the lights go on) are plotted against N. It can be easily seen that the ratio of specific activities of polyribosomes of sizes 9 and 6 increases between 4.5 and 11 h and decreases between 11 and 18.5 h. The ratios at different times throughout the cell cycle from a number of separate experiments are plotted in Figure 7A. These ratios have been used to calculate the peptide interval times in panel B using the relationship in Figure 5. Panel B shows that the peptide interval time, I, does not change dramatically during the cell cycle. At most, there is a twofold change in I, which drops from about 8 to about 4 s during the light period of the cycle and rises in the dark period after the time of cell division (ca. 16 h). The relationship between peptide interval time and elongation rate (panel C) will be described under Discussion.

Recruitment of Ribosomes into Polyribosomes. The number of ribosomes in polyribosomes (P) depends on the balance between the rates of polypeptide chain elongation, chain initiation, and accumulation of new ribosomes. Thus, if the rates of chain elongation and ribosome accumulation are known, P can be used to determine the chain initiation rate. We have measured the proportion of ribosomes in polyribosomes, p, at various cell-cycle stages. The value of p was measured for both cytoplasmic and chloroplastic polyribosomes by determining

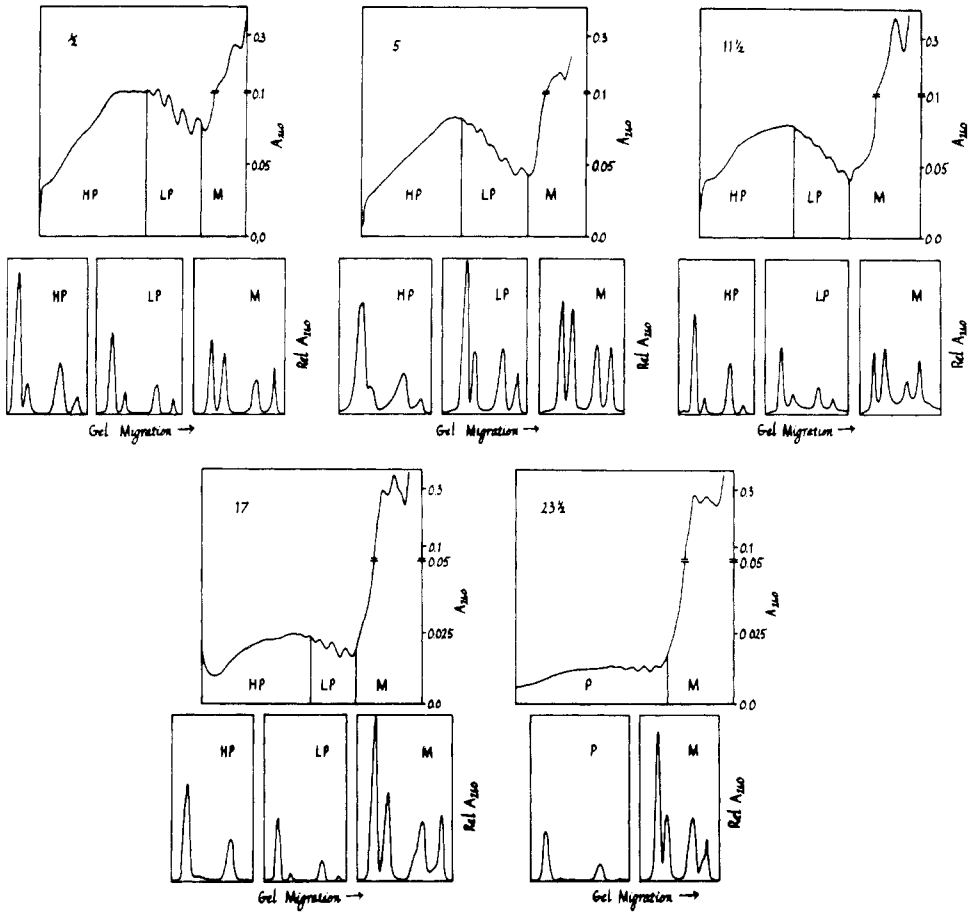

FIGURE 8: Ribosomal RNA from polyribosome fractions at different cell-cycle stages. Polyribosomes were extracted from synchronized cells at the times indicated. Upper panel in each group shows the optical density (A_{260}) profile of polyribosomes obtained upon centrifugation of whole-cell lysates on sucrose density gradients (sedimentation is from right to left), and lower panels in each group show the composition of ribosomal RNA extracted from pooled gradient fractions and analyzed by electrophoresis of polyacrylamide gels. Two classes of polyribosomes were analyzed (except at 23.5 h when there was not enough polyribosomal material), designated HP, large or heavy polyribosomes ($N > 6$), and LP, small or light polyribosomes ($N < 6$). M designates material in the "monosome region" composed primarily of ribosomal subunits dissociated in the high salt. The four peaks in the ribosomal RNA profiles represent (from right to left) 16S, 18S, 23S, and 25S ribosomal RNA species. The 16S and 23S chloroplast ribosomal RNAs comigrate with *E. coli* marker ribosomal RNA. The ribosomal RNA profiles were obtained by scanning gels at 260 nm, and the ordinates in the gel profiles represent relative optical density.

the amount of chloroplast (16 and 23 S) and cytoplasmic (18 and 25 S) ribosomal RNA in monoribosome and polyribosome fractions of polyribosome gradients. The data from five cell-cycle stages is presented in Figure 8. This figure shows profiles of polyribosome sucrose density gradients and of polyacrylamide gels of ribosomal RNA from monoribosomal and polyribosomal fractions. Several aspects of polyribosome behavior during the cell cycle can be observed. First, at all cell-cycle stages, polyribosomes are composed predominantly of cytoplasmic ribosomes (18S and 25S RNA). Second, only at the very beginning of the light period (30 min) are there many chloroplast ribosomes among the large or heavy polyribosomes, and thus, when the light period begins, there is a sizeable shift of chloroplast ribosomes into large or heavy polyribosomes. Third, during the light period, the overall proportion of ribosomes in polyribosomes remains fairly constant, but this proportion declines in the dark period. This is shown more clearly in Figure 9, where values of p for total ribosomes (panel A) and for cytoplasmic and chloroplastic ribosomes (panel B) are plotted as a function of cell-cycle stage. Values of p for total and cytoplasmic ribosomes remain constant during the light period, while p declines somewhat for chloroplastic ribosomes during that period. The values of p for total and cytoplasmic ribosomes decrease after the light–dark transition (at 12 h) and rise sharply for both ribosomal species at the dark–light transition (0 or 24 h). Thus, at the beginning of the light period, there is a rapid recruitment of both cytoplasmic and chloroplastic ribosomes into polyribosomes, and, at that stage, and only briefly at that stage, large chloroplast polyribosomes are found.

Discussion

In this study, we have determined rates of protein synthesis during the cell cycle by a method in which one measures the separate rates of polypeptide chain initiation and elongation. To measure chain-elongation rates, we used a scheme modified from Enger and Tobey (1972) for comparing the rate of labeling of nascent polypeptide chains in two size classes of polyribosomes. This has been done by determining the ratios of specific activities of polyribosomes of $N = 6$ and $N = 9$ following 30-s pulse labeling with [^{3}H]arginine at different times during the cell cycle. The method is unaffected by possible precursor-pool specific-activity problems because it is based on a comparison of the rates of labeling of two different classes of polyribosomes which are presumably drawing from the same radioactive precursor pool. These ratios of polyribosome specific activities during the cell cycle have been used to calculate peptide interval times, I, as shown in Figure 7B. I varies only

about twofold during the cell cycle, from about 8 to 9 s at the end of the dark period and the beginning of the light period to about 4 s beginning at the light–dark transition and for about half of the dark period.

We have used the values of I to determine the relative polypeptide chain elongation rate (amino acids added per peptide chain per unit of time). The chain elongation rate, r_e, is inversely related to I according to the following relationship:

$$r_e = c/I \quad (1)$$

where c, an undetermined constant in this system, is the number of amino acids in a peptide interval unit. Thus, the relative chain-elongation rate during the cell cycle (shown in Figure 7C) is the inverse of the peptide interval time. In synchronized *C. reinhardi*, the chain-elongation rate rises during the light period and falls off after remaining high for a few hours in the dark period. The elongation rate begins to drop near the time of cell division at about 16 h (see Figure 1). The changes in the relative elongation rate described here pertain only to cytoplasmic polyribosomes, since we have measured specific activity ratios on intermediate-sized polyribosomes which are composed almost entirely of cytoplasmic polyribosomes (Baumgartel and Howell, 1976a).

To determine changes in the initiation rate during the cell cycle, we have used several types of data from different cell-cycle stages to calculate P, the number of ribosomes per cell in polyribosomes. We have defined the initiation rate, r_i, to be the number of polypeptide chain-initiation events *per cell* per unit time. As discussed earlier, P is influenced by both r_i and r_e. It increases with increasing r_i and decreases with increasing r_e; that is,

$$P = m(r_i/r_e) \quad (2)$$

where m is a parameter which relates to the size distribution of messenger RNAs being translated. Equation 2 shows the effects of r_i and r_e on P if r_i and r_e are independent. Vassart et al. (1971) have generated values of p, the proportion of ribosomes in polyribosomes, using a Monte-Carlo computer simulation of protein synthesis on a homogeneous messenger RNA population and changing r_e and r_i. They found a 70% increase in p for a 100% increase in r_i and a 40% decrease in p for a 100% increase in r_e. The difference between their results and the expectations described in eq 2 is that the computer simulation includes situations in which r_i and r_e are rate limiting on the other. This interdependence is caused by the heavy packing of polyribosomes which might block initiation sites on mRNA molecules or might restrict the movement of ribosomes.

We have not dealt with this interdependence because we find no gross changes in polyribosome packing density during the cell cycle; that is, the size distributions of polyribosomes are nearly the same at different cell-cycle stages (Figure 8). This latter observation also suggests that the parameter m in eq 2, which relates to the size distribution of the messenger RNA population being translated, does not change appreciably with cell-cycle stage. Our unpublished observations also indicate that the size distribution of newly synthesized, released polypeptide chains does not change significantly during the cell cycle. Thus, m can be regarded as a constant, and it is canceled in the calculation of relative changes in rate during the cell cycle.

To calculate r_i, eq 2 is rearranged as

$$r_i = Pr_e/m \quad (3)$$

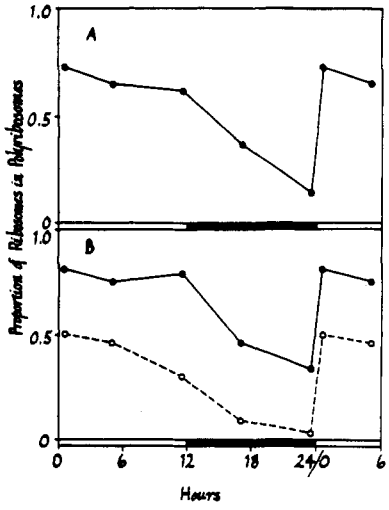

FIGURE 9: Proportion of ribosomes found in polyribosomes (p) at different cell-cycle stages using data of Figure 8. Panel A shows p for both ribosome types. Panel B shows the proportion of cytoplasmic ribosomes (●—●) and chloroplastic ribosomes (○ - - - ○) found in polyribosomes. Chloroplastic ribosomes are represented by 16 and 23S ribosomal RNA and cytoplasmic ribosomes by 18 and 25S ribosomal RNA in Figure 8.

At any cell-cycle stage, P, the number of ribosomes in polyribosomes, is related to p, the (fractional) proportion of ribosomes in polyribosomes, as follows:

$$P = Adp \quad (4)$$

where A is the amount of ribosomal RNA per cell and d is a constant relating the amount of ribosomal RNA to the number of ribosomes. We have taken values of A from the data from Cattolico et al. (1973) for different cell-cycle stages (for either cytoplasmic or chloroplastic ribosomal RNAs). By substituting eq 1 and 4 into eq 3, r_i can be expressed as a function of experimentally determined values as:

$$r_i = fAp/I \quad (5)$$

where the new parameter f is substituted for dc/m. Calculated values of r_i using A for cytoplasmic ribosomal RNA represent initiation rates on cytoplasmic polyribosomes, since I has been obtained only for cytoplasmic polyribosomes. Also, values of r_i will be relative, since the combined parameter f is undetermined, though constant, at different cell-cycle stages.

Using the relationship in eq 5 with the values we have obtained for p and I, as well as values of A from Cattolico et al. (1973), we have calculated the relative changes in the initiation rate on cytoplasmic polyribosomes during the cell cycle. A plot of the calculated r_i values is shown in Figure 10. The figure shows that r_i varies greatly during the cell cycle, about 25–50-fold. Although the increase in the initiation rate is slight at the very beginning of the light period, it is sufficient to cause recruitment of a high proportion of the existing cytoplasmic ribosomes into polyribosomes, since both the amount of ribosomes and the elongation rate are low at that time. After that, in the light period, the increasing r_i keeps pace with the accumulation of newly synthesized ribosomes (about a fourfold increase) and increasing r_e (about a twofold increase) to maintain a nearly constant proportion of ribosomes in polyribosomes. The initiation rate drops to its initial low level by about halfway through the dark period (18 h), and, since r_e remains at a relatively high level during that time, polyribosomes disassemble.

The changes in the overall rate of protein synthesis, r_s (amino acids added per cell per unit time), can be calculated

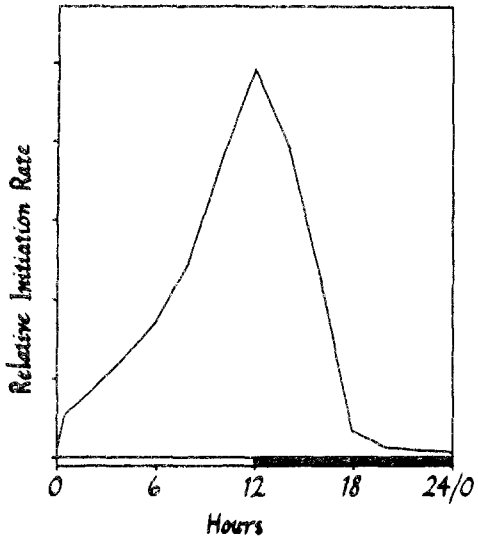

FIGURE 10: Changes in the relative chain initiation rate (r_i) during the cell cycle. Initiation rates were calculated according to eq 5. See text for explanation.

from the separate values described above. The rate of protein synthesis per cell is the product of the number of growing nascent chains per cell (the number of active ribosomes in polyribosomes per cell (P)) and the rate of elongation (r_e); that is,

$$r_s = Pr_e \quad (6)$$

We have shown earlier that $P = m(r_i/r_e)$ (eq 2). Thus,

$$r_s = mr_i \quad (7)$$

Since m is constant throughout the cell cycle, r_s changes directly with r_i, and, therefore, Figure 10 shows relative changes in the rate of protein synthesis during the cell cycle, as well as changes in r_i.

The changes in the rate of overall protein synthesis (either cytoplasmic or chloroplastic) are not related to events in the cell cycle in the manner previously expected. The rate of protein synthesis does not fall at the time of cell division (ca. 16 h), recover immediately thereafter, and remain constant throughout the remainder of the cell cycle. Instead, the rate seems to depend on the light–dark illumination cycle. Rates of chain initiation and protein synthesis rise during the light period and fall when the lights go off. On the other hand, the chain-elongation rate shows a different pattern. It rises during the light period but does not fall immediately after the lights go off, falling only later, about halfway through the dark period. The regulation of the initiation rate during the light period is quite remarkable, since the increase in rate means that a high proportion of cytoplasmic ribosomes is maintained in polyribosomes during a period when both the number of ribosomes per cell and the polypeptide chain elongation rate are increasing. The rate of protein synthesis falls off rapidly in the dark period; nevertheless, the rate of protein synthesis at any time during the first half of the dark period is considerable. This is an interesting observation compared with the findings of Kates and Jones (1964) who showed that the accumulation of total protein is restricted to the light period. During the dark period, therefore, the rate of protein degradation must equal the rate of protein synthesis and must be high.

In this study, we have dealt primarily with changes in the rate of protein synthesis on cytoplasmic polyribosomes. We have not been able to measure chain initiation and elongation rates directly on chloroplast polyribosomes; however, from the distribution of chloroplast ribosomes in polyribosome profiles, we can make some statements about the changes in initiation rate relative to changes in elongation rate on chloroplast polyribosomes during the cell cycle. At the beginning of the light period, the proportion of chloroplast ribosomes in polyribosomes rises sharply, as does the average size of chloroplast polyribosomes. This indicates that the initiation rate on chloroplast polyribosomes rises rapidly relative to the elongation rate at that time. During the remainder of the light period, the initiation rate fails to keep pace with both the synthesis of new chloroplast ribosomes (Cattolico et al., 1973) and apparent ongoing elongation rates, so that both the proportion of chloroplast ribosomes in polyribosomes (Figure 8) and the average size of chloroplast polyribosomes decline.

The changes in the rate of protein synthesis on cytoplasmic polyribosomes during the cell cycle are much greater than the changes in the rate of whole cell [^{3}H]arginine incorporation (Figure 3). The rate change for incorporation is only five- to tenfold, while the change in the rate of protein synthesis is 25–50-fold. As suggested earlier, the differences between changes in rates of incorporation and synthesis are most likely due to differences in arginine pool specific activity during pulse labeling at different times in the cell cycle. It is unlikely that the differences arise from the contributions by chloroplast polyribosomes to the total cellular rate of protein synthesis. First, the cell-cycle pattern of initiation-rate changes on chloroplast polyribosomes as discussed above is quite similar to initiation-rate changes on cytoplasmic polyribosomes, and so during the cell cycle, for example, initiation rates on chloroplast polyribosomes do not rise to compensate for falling rates on cytoplasmic polyribosomes. Second, although chloroplast ribosomes constitute about 30% of the total cellular ribosomes in *C. reinhardi* (Hoober and Blobel, 1969; Baumgartel and Howell, 1976a), they contribute surprisingly little to overall protein synthesis in the cell. The principal product of the chloroplast protein-synthesizing machinery in *C. reinhardi* is the large subunit of the CO_2-fixation enzyme, D-ribulose-1,5-bisphosphate carboxylase (EC 4.1.1.39) (Hoober, 1972). This polypeptide constitutes about 5–7% of the total cellular protein (Howell et al., 1977). Therefore, when one considers the synthesis of this polypeptide plus the other chloroplast-produced proteins, a better estimate of the output from chloroplast polyribosomes is probably about 10% of the total cellular protein.

It has been argued that chloroplast ribosomes are inefficient at protein synthesis on a per ribosome basis because initiation rates on chloroplast polyribosomes are slow (Baumgartel and Howell, 1976a). This is certainly supported by the data in Figure 8 which show that, even at cell-cycle stages when the output from chloroplast polyribosomes is thought to be high (midlight phase), the proportion of chloroplast ribosomes in polyribosomes is low and the size of chloroplast polyribosomes is small, suggesting a low packing density (Figure 8). The synthesis of the large subunit of the CO_2-fixation enzyme is a case in point. This chloroplast-produced polypeptide is relatively large, molecular weight 55 000 (Iwanij et al., 1975; Gelvin and Howell, 1977); however, it is synthesized on small chloroplast polyribosomes (Gelvin and Howell, 1977). If initiation rates were as high on chloroplast polyribosomes as on cytoplasmic ones, than one might expect that this polypeptide would be synthesized on much larger polyribosomes, i.e., polyribosomes with a higher packing density (Gelvin and Howell, 1977). Thus, we suggest that chloroplast polyribosomes contribute little to the overall rate changes of protein synthesis

during the cell cycle, simply because they contribute little to the overall synthesis of cellular protein in *C. reinhardi*.

Changes in the rate of protein synthesis during the cell cycle may result from general changes in the physiology of the cell or from specific changes in a component, or in components, of the protein-synthesizing apparatus. Changes in elongation rate could be due to changes in the amounts of elongation factors, aminoacyl-tRNAs and their binding factors, and/or GTP. Preliminary experiments with a *C. reinhardi* cell-free system using materials derived from cells at different cell-cycle stages suggest that changes in soluble elongation factors may contribute significantly to the changes in elongation rate during the cell cycle (data not shown). The somewhat more dramatic changes in the initiation rate during the cell cycle could be due to changes in the amounts of mRNA, initiation factors, initiator aminoacyl-tRNA, ribosomal subunits, and/or GTP. We have not yet determined what these changes are.

There are several indications that changes in the rate of polypeptide chain initiation during the cell cycle may be the most important translational control for regulating the rate of synthesis of specific proteins during the cell cycle in *C. reinhardi*. First, as shown above, changes in the initiation rate govern changes in the overall rate of protein synthesis during the cell cycle. Second, changes in the initiation rate may also exert qualitative controls affecting the patterns of polypeptides synthesized at any cell-cycle stage. An example of this effect has been recently described by Lodish (1974). He has shown that changes in initiation rates can alter the relative rates of synthesis of α- and β-globin in reticulocyte extracts. The shift has been attributed to competition between the two types of messenger RNAs for the formation of initiation complexes. The vast differences in initiation rates seen during the cell cycle of *C. reinhardi* must have some effect on the selection of messenger RNAs to be synthesized at different cell-cycle stages.

References

Baumgartel, D. M., and Howell, S. H. (1976a), *Biochim. Biophys. Acta 454*, 338–348.

Baumgartel, D. M., and Howell, S. H. (1976b), *Biochim. Biophys. Acta 454*, 349–361.

Beck, D. P., and Levine, R. P. (1974), *J. Cell Biol. 63*, 759–772.

Bourguignon, L. Y. W., and Palade, G. E. (1976), *J. Cell Biol. 69*, 327–344.

Brewer, E. N. (1972), *Biochim. Biophys. Acta 277*, 639–645.

Cattolico, R. A., and Jones, R. F. (1972), *Biochim. Biophys. Acta 269*, 259–264.

Cattolico, R. A., Senner, J. W., and Jones, R. F. (1973), *Arch. Biochem. Biophys. 156*, 58–65.

Enger, M. D., and Tobey, R. A. (1972), *Biochemistry 11*, 269–277.

Fan, H., and Penman, S. (1970), *J. Mol. Biol. 50*, 655–670.

Gelvin, S., and Howell, S. H. (1977), *Plant Physiol. 59*, 471–477.

Hoober, J. K. (1972), *J. Cell Biol. 52*, 84–96.

Hoober, J. K., and Blobel, G. (1969), *J. Mol. Biol. 41*, 121–138.

Howell, S. H., Heizmann, P., Gelvin, S., and Walker, L. L. (1977), *Plant Physiol. 59*, 464–470.

Howell, S. H., Posakony, J. W., and Hill, K. R. (1977), *J. Cell Biol. 72*, 223–241.

Iwanij, U., Chua, N.-H., and Siekevitz, P. (1975), *J. Cell Biol. 64*, 572–585.

Johnson, T. C., and Holland, J. J. (1965), *J. Cell Biol. 27*, 565–574.

Kates, J. R., and Jones, R. F. (1964), *Biochim. Biophys. Acta 145*, 153–158.

Kuff, E. L., and Roberts, N. E. (1967), *J. Mol. Biol. 26*, 211–225.

Lodish, H. F. (1974), *Nature (London) 351*, 385–388.

Loening, U. E. (1969), *Biochem. J. 113*, 131–138.

Mitchison, J. M. (1971), The Biology of the Cell Cycle, Cambridge, Cambridge University Press.

Mittermayer, C., Braun, R., Chayka, T. G., and Rusch, H. P. (1966), *Nature (London) 210*, 1133–1137.

Morton, B. (1974), *Anal. Biochem. 58*, 642–645.

Reisner, A. H., Askey, C., and Aylmer, C. (1972), *Anal. Biochem. 46*, 365–373.

Steward, D. L., Schaeffer, J. R., and Humphrey, R. M. (1968), *Science 161*, 791–793.

Sueoka, N., Chiang, K. S., and Kates, J. R. (1967), *J. Mol. Biol. 25*, 47–66.

Vassart, G., Dumont, J. E., and Cantraine, F. R. L. (1971), *Biochim. Biophys. Acta 247*, 471–485.